16th World Conference on Earthquake Engineering, 16WCEE 2017

Santiago Chile, January 9th to 13th 2017

Paper N° 1576

Registration Code: S-P1464691111

AFTERSHOCK COLLAPSE VULNERABILITY ASSESSMENT OF AN OLDER REINFORCED CONCRETE FRAME

M. Raghunandan[(1)], A. Liel[(2)]

[(1)] *Assistant Professor, Dept. of Civil Engineering, IIT Bombay, India, meerar@iitb.ac.in*

[(2)] *Associate Professor, Dept. of Civil, Environmental and Architectural Engineering, University of Colorado Boulder abbie.liel@colorado.edu*

Abstract

Buildings located in seismically-active regions may experience ground shaking from multiple earthquakes, such as mainshock-aftershock sequences. In mainshock-aftershock sequences, the seismic events generally occur in close succession, leaving insufficient time for repair or retrofit between the events. In such cases, seismic performance of a building during an aftershock may depend on the level of damage sustained by the building in mainshock. This study evaluates the aftershock collapse vulnerability of a non-ductile reinforced concrete moment frame building designed according to the 1967 Uniform Building Code. This type of reinforced concrete moment frames is relatively weak, and susceptible to shear and axial column failure (among other failure modes) due to inadequate reinforcement detailing and lack of capacity design requirements. Here, the reinforced concrete frame is modeled in two dimensions with zero-length springs on top of columns capable of capturing shear and axial failure modes. Incremental dynamic analysis on nonlinear analytical building models is used to generate damage and collapse fragility curves for intact and mainshock damaged buildings. The results show that the structure's ability to withstand collapse and further damage are decreased as the extent of damage after the mainshock increases. This trend is similar to what has been observed for ductile RC frames. However, a modern ductile RC frame can undergo higher levels of damage before its aftershock collapse capacity is seriously compromised. In addition, the drop in collapse capacity, as a function of mainshock damage, is more precipitous for the non-ductile RC frame building.

Keywords: aftershocks; non-ductile reinforced concrete buildings; collapse; residual capacity

1. Introduction

In a seismically active region, buildings may be exposed to multiple earthquakes within a fairly short period of time. In a mainshock-aftershock scenario, a building is subjected to shaking from a major earthquake or "mainshock" and then subjected to shaking from other smaller magnitude earthquakes originating at or near the mainshock rupture zone, which are commonly referred to as "aftershocks". For example, in the Tohuku earthquake in Japan (M_w 9, 2011), buildings were subjected to large magnitude mainshock, and several hundred aftershocks with magnitudes up to M_w 7.9 within the first year of mainshock [1]. Generally, mainshock and aftershocks occur in close succession, leaving insufficient time between the events for repair and retrofit of the mainshock damaged buildings. This may result in accumulation of damage in the building over an earthquake sequence. In addition, there may be a significant reduction in the capacity of a building damaged in mainshock to withstand subsequent shaking from aftershock.

A number of studies have been conducted to assess the performance of structures subjected to earthquake sequences. All of these studies have generally concluded that structures experience more damage when subjected to earthquake sequences, such as mainshock-aftershock sequences, as compared to shaking from a single event [2]–[4]. This increased vulnerability of buildings to damage in aftershocks can be explained by the increased duration of shaking the building is subjected to when shaken by aftershocks as well as mainshocks. Raghunandan and Liel [5] evaluated the effect of ground motion duration on collapse of reinforced concrete (RC) moment frame buildings and found that both non-ductile and ductile buildings have lower collapse capacities (resistance against earthquake-induced collapse) when subjected to a long duration ground motion (or sequence) as compared to a short duration ground motion with same intensity. More recently, Raghunandan *et al.* [6] quantified the aftershock vulnerability of four modern ductile RC frame buildings in California. They generated collapse and damage fragility curves for buildings in the intact condition, and in varying levels of damage in the mainshock. This assessment was conducted though incremental dynamic analysis by subjecting nonlinear multiple-degree-of-freedom numerical models of buildings to mainshock-aftershock sequences. The study indicated that if the buildings were not severely damaged in mainshock, their aftershock collapse capacity was not substantially affected. However, if the building experienced extensive damage in mainshock, capacity to resist collapse in subsequent shaking is significantly reduced. The buildings considered in Raghunandan *et al.* [6] were all modern, seismically-detailed special moment resisting frames.

This study extends these findings to consider an older non-ductile RC moment frame building. This building type is prevalent in U.S. high seismic regions and elsewhere around the world. These buildings are known to be more vulnerable to collapse as compared to their modern ductile counterpart because of their lower strength and ductility, and possible loss of gravity-load bearing capacity in columns, as well as other brittle failure modes [7]. For example, during the 2010-2011 Christchurch earthquake sequence in New Zealand, extensive damage and collapse were observed for a number of non-ductile RC buildings [8]. To corroborate these observations, Raghunandan *et al.* [9] subjected a non-ductile 4-story frame building representative of mid-century New Zealand construction to 900 artificial earthquake sequences and observed that extensive damage in first event can significantly reduce the collapse capacity of the building for future shaking. This study evaluates the aftershock collapse vulnerability of a non-ductile RC moment frame building designed according to 1967 Uniform Building Code for the highest seismic hazard level in the U.S. at the time (*i.e.*, California). The RC frame is modeled as a two-dimensional multiple-degree-of-freedom model. The column modeling approach is capable of capturing shear and axial failure modes using state-of-the-art modeling techniques (*e.g.* [10]), significantly improving the modeling approach for non-ductile frames from author's previous study [9]. Incremental dynamic analysis is used to generate aftershock damage and collapse fragility curves for intact and mainshock damaged buildings. The results are developed to quantify the reduction in collapse capacity of the structure in aftershock depending on the level of damage sustained by the building in mainshock. These fragility curves are then compared with aftershock fragility curves for the similar RC frame designed according to modern building codes from Raghunandan *et al.* [6].

2. Buildings and Building Models

This study explores the aftershock vulnerability of non-ductile RC buildings, which perform differently under seismic loading than the ductile reinforced concrete buildings previously evaluated by Raghunandan *et al.* [6]. These buildings have lower strength and deformability than their ductile and modern counterparts. In particular, low and poor transverse reinforcement detailing makes them susceptible to brittle shear and axial failure in load bearing columns. In contrast, modern RC frames, also known as "special" moment resisting frames, satisfy requirements of strong-column-weak-beam design, shear capacity design and detailing requirements. These provisions significantly increase the deformation capacity of the modern ductile buildings, and ensure that the global failure of these buildings occurs due to flexural failure of the elements in a sidesway mechanism.

This study examines a 4-story non-ductile RC moment resisting frame designed according to the 1967 Uniform Building Code for high seismic zones. The building is modelled analytically in *OpenSees* [11] as two-dimensional, three-bay space frame, as illustrated in Fig. 1. To capture collapse, the nonlinear model should be capable of simulating different modes of strength and stiffness degradation during the course of earthquake shaking that lead to structural collapse. To this end, the flexural behavior of the beam and columns is modelled using lumped-plasticity beam column elements (ZL Type II, Fig. 1). The plastic hinges that describe the flexural behavior of the beam column members are modelled using the hysteretic material developed by Ibarra *et al.* [12] that is capable to simulating flexural strength and stiffness deterioration of beam-columns under dynamic loading, as well as bond slip deformations. The non-ductile RC columns are susceptible to brittle shear and axial failure in addition to flexural failure. The possible occurrence of column shear failure (occurring either before or after column yielding) and axial failure is captured by use of a zero length element provided on top of column consisting of uniaxial shear and axial springs coupled with flexural rotational spring (ZL Type I, Fig. 1). These axial and shear springs are assigned the so-called limit state material developed by Elwood [10] in combination with Sezen and Moehle's [13] shear strength model. The shear (or axial) spring tracks the flexural response of the associated column and detects shear (or axial) failure as occurring when the column force-displacement relationship crosses the shear (or axial) limit state curve for the column. The limit state curve for a column depends on its material, axial load and detailing properties. Once these shear (or axial) failures modes are identified for a column, the shear (and axial) response is updated and a softening response occurs. Since shear and axial failures are brittle modes of failure, they occur low drift levels compared to flexural model of failure of columns. More information about the building and the associated model can be found in Raghunandan *et al.* [14], in which the authors have used the same model for a different study.

In these structural analysis models, collapse can occur in one of two modes. The first, termed as shear collapse mode, occurs if the total lateral strength of all columns in a story degrades beyond the total residual capacity of columns. This degradation stems from a combination of shear and flexural response axial collapse mode which occurs if the total axial load carrying capacity of a story is exceeded by the total gravity load demand on the story. This procedure is described in more detail by Raghunandan *et al.* [14]. in columns. The second mode is

The pushover response of the 4-story non-ductile moment frame is plotted in Fig. 2. The structure has an eigenvalue first-mode period of 1.11s (considering cracked sections for beams and columns), and an ultimate capacity of 160 kips, representing an overstrength of 2.7 in relation to the design base shear of 60 kips. The pushover analysis illustrates the strength of the structure and the range of lateral displacement the structure can experience. In this case, a shear failure mechanism is initiated for one of the columns at 1.7% interstory drift. At higher drifts, softening of the pushover (reduction in strength for increased loads) is expected to occur, however due to challenges with convergence, the response is not plotted here. In Fig. 2, the pushover curve for modern 4-story reinforced concrete moment frame building by Haselton *et al.* [15] is also shown alongside the non-ductile frame pushover results. The modern 4 story ductile space frame has first-mode period of 0.91s and ultimate capacity of 230 kips (design base shear of 86 kips). Also, the modern building retains significant ductility capacity at 1.7% drift; indeed, it can sustain close to 6% drift in the pushover before experiencing a negative slope. Although the structure is designed for the same high-seismic site as the modern comparison structure, Fig. 2 shows that the non-ductile building has less strength and substantially less ductility than the code-conforming structure. These differences can be attributed to the myriad seismic design and detailing requirements that essentially move beyond a force-based approach in modern codes.

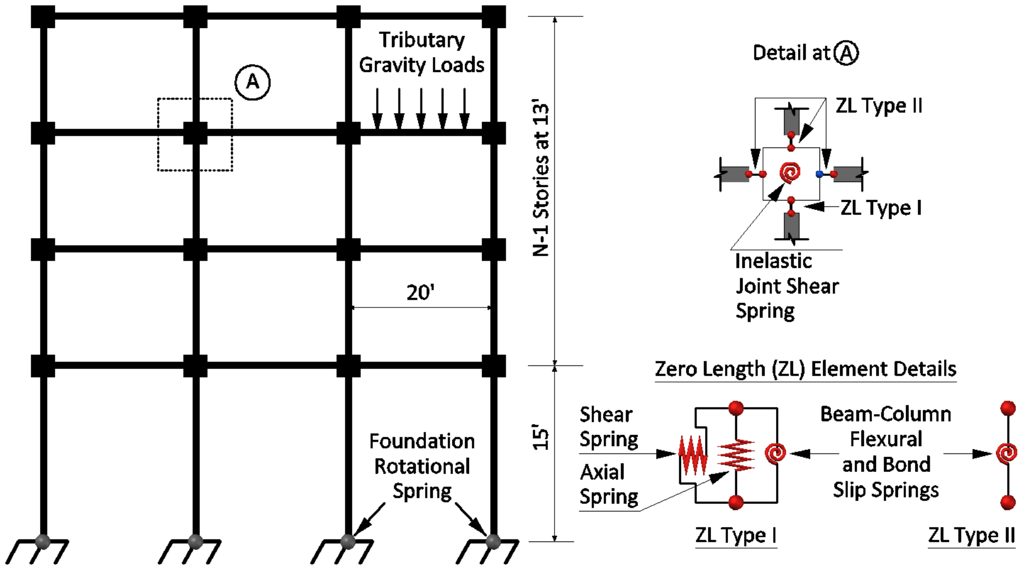

Fig. 1 – Graphical representation of the analytical building model [14].

The response of the structure and its capacity to carry subsequent seismic loads varies depends on the level of damage sustained by the building in mainshock. The mainshock damage sustained by the building can be quantified using a number of structural response parameters, such as maximum or residual interstory drift ratio, maximum or residual roof ratio [6]. In this paper, mainshock damage is measured using the maximum interstory drift ratio experienced by the building during mainshock. Maximum interstory drift ratio can serve as a convenient proxy to structural damage because it is highly correlated to structural damage and repair costs, e.g. [16]. Raghunandan *et al.* [6] found that the collapse capacity of the building is significantly affected by mainshock damage if it experiences an extensive amount of damage in mainshock; for ductile frames, this extensive damage corresponds physically to 3% to 5.5% maximum interstory drift ratio. However, for this non-ductile building, 1.5%-2% drift itself may correspond to extensive damage state, as shear failure mechanism was initiated for some non-ductile columns at 1.7% drift level in static pushover analysis. Therefore, in this study, four levels of mainshock damage based on maximum interstory drift are considered for assessment of aftershock collapse risk. The predefined levels of damage sustained by the building can also be referred to as damage states and in this study, they correspond to maximum interstory drift ratios in mainshock of: (a) 0.5% (DS1), (b) 1% (DS2), (c) 1.5% (DS3) and (d) 2% (DS4). For example, DS1 corresponds to the structure experiencing a maximum (transient) interstory drift ratio of 0.5% during the mainshock. Physically, these damage states cover behavior ranging from from slight (DS1) to extensive (DS4) damage.

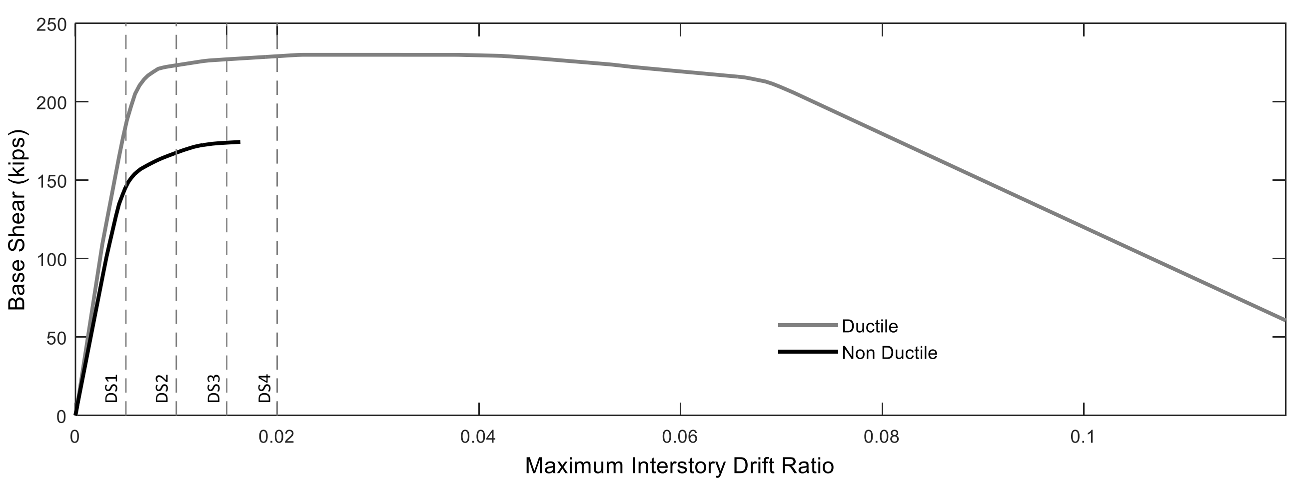

Fig. 2 – Nonlinear pushover analysis results for modern ductile and older non-ductile 4-story buildings. The dotted lines in the plot indicate the levels of mainshock damage considered in the study.

3. Nonlinear Dynamic Analysis

3.1 Overview

The analytical building models are subjected to a suite of recorded ground motions for dynamic analysis. The ground motions used have been compiled by Vamvatsikos and Cornell [17], and consist of records from earthquakes with magnitude (M_w) between 6.5 and 6.9, and recorded at sites with closest distance to fault rupture between 15 and 33km. These ground motions represent seismicity of California, where the buildings of interest are located. Here, these records are used to represent both aftershocks and mainshocks, despite evidence that frequency content may be dissimilar for both seismic events [18].

The dynamic procedure can be divided into two parts: (a) Mainshock analysis or IDA of intact building, and, (b) Aftershock analysis or IDA of damaged building. In IDA, a ground motion is applied to the structure and dynamic response is simulated and recorded. The same ground motion is then scaled and applied to the structure again, repeating the analysis at a higher ground motion intensity level. This procedure is continued until the scaled record causes the collapse of the structure according to the shear and axial failure collapse criteria described above. In this study, ground motion intensity is measured using inelastic spectral displacement. Inelastic spectral displacement is the maximum displacement of a single-degree-of-freedom oscillator when subjected to the ground motion of interest. The oscillator has a period corresponding to the building of interest. The force-displacement response of the oscillator is bilinear, defined by a yield displacement (equal to yield displacement of building of interest) and 5% hardening stiffness [19]. Since record selection and spectral shape have been shown to have an important influence on structural collapse, we use inelastic spectral displacement rather than the more conventional spectral acceleration to achieve an intensity measure that reflects both ground motion intensity and spectral shape in its valuation [20].

3.2 Mainshock analysis

The dynamic analysis procedure begins with IDA of intact building (no mainshock damage), which is used to predict the collapse capacity of the intact structure. The mainshock IDA results for the non-ductile and ductile RC moment frames considered in this study are provided in Fig. 3. The collapse capacity of an intact structure for a particular ground motion is defined as the intensity measure of the scaled mainshock ground motion (in terms of S_{di}) that causes the collapse of the structure. The collapse capacities of the building generally follow a lognormal distribution that can be defined using two parameters, median and lognormal standard deviation. The median collapse capacity provides a measure of the average intensity of ground motion the structure can withstand before collapse occurs and it represents the intensity of ground motion, corresponding to 50% probability of collapse of building. For the non-ductile and ductile 4-story buildings, the median collapse capacities are 6in. and 11in. respectively, clearly indicating the superior collapse resistance of ductile buildings. Fig. 3 also reveals that the maximum drifts experienced by the non-ductile building (2-3.5%) at collapse are significantly lower than its modern ductile building counterpart (>8%). The record-to-record variability in collapse capacity is quantified as using the lognormal standard deviation of the collapse capacity distribution, which is 0.19 and 0.30 for non-ductile and ductile buildings, respectively. The higher standard deviation of ductile buildings occurs because of the highly nonlinear response that can occur before collapse in the ductile building case, providing many possible paths to collapse.

In this study, we are interested in four mainshock damage states, corresponding to interstory drift ratios of 0.5%, 1%, 1.5% and 2%. The mainshock analysis is used to determine the scale factors needed to be applied to each motion to achieve this damage state under the first, mainshock motion in preparation for the aftershock analysis.

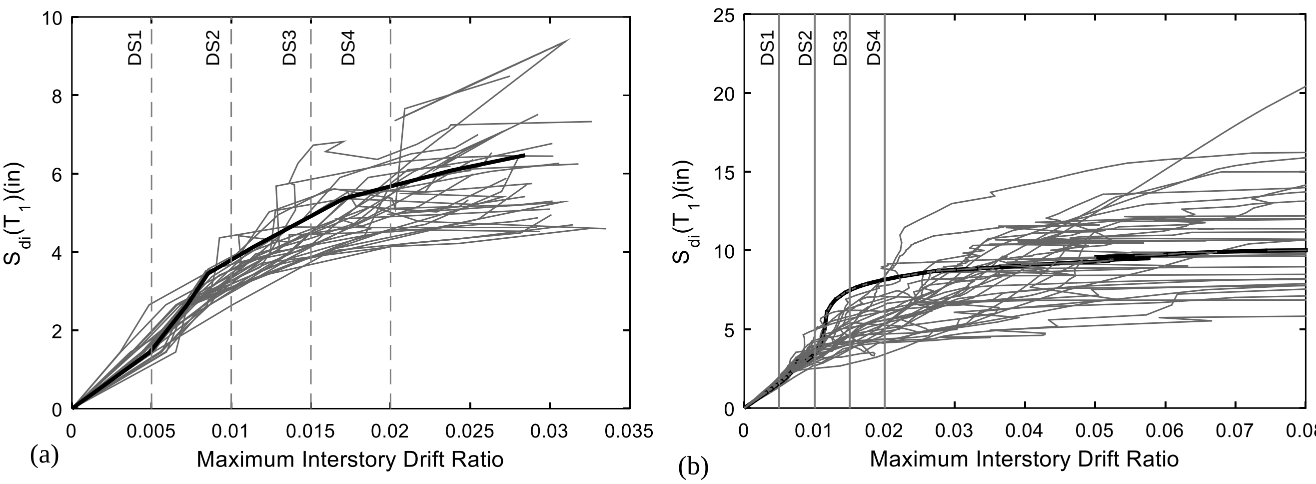

Fig. 3 – Incremental dynamic analysis results of the (a) 4-story intact non-ductile RC frame building and (b) 4-story intact ductile RC frame building, wherein the bold line highlights IDA results from one of the 30 ground motions.

3.3 Aftershock analysis

The aftershock analysis consists of IDA on the damaged building, as defined by the damage state of interest. Aftershock IDA results provide the collapse capacity of a building damaged to a particular damage state in the previous mainshock event. This aftershock collapse capacity can be interpreted as a measure of residual capacity of the mainshock damaged building to sustain future shaking. The assessment of the structure in the damaged condition requires running a sequence of mainshock and aftershock ground motions. Here, we first scale one of the records - treated as a mainshock - by a factor to simulate the mainshock damage state of interest for the building as described above. After allowing time for the building model to come to rest in the analysis (4s in this case), the now damaged structure is subjected to a selected record as an aftershock, as shown in Fig. 4. This sequence is repeated, with increasing scale factor on the aftershock record until collapse occurs. The collapse capacity of the damaged building is quantified by the intensity of the scaled aftershock ground motion causing collapse of structure. This process requires running each of the 30 records as mainshocks in combination with all 30 records as aftershocks, corresponding to 900 analyses per damage state, resulting in a total of 900 x 4 = 3600 aftershock analyses for each building.

4. Aftershock Analysis Results

4.1 Aftershock dynamic analysis results

Aftershock IDA results for the mainshock-damaged 4-story non-ductile building for one of the damage states (ISD 0.015, DS3) are illustrated in Fig. 5. The x-axis represents the maximum interstory drift experienced by the structure during the whole mainshock-aftershock sequence; the y-axis represents the intensity measure of scaled aftershock ground motion in the sequence. During IDA, at low intensities of aftershock shaking, the maximum interstory drift ratio for sequence will be controlled by the maximum drift experienced by the structure during the first (mainshock) ground motion corresponding to the damage state of interest. This feature explains why there is a vertical line in the IDA plots in Fig. 5, where maximum drift is constant when the intensity of aftershock ground shaking is low. The drift value at low intensity measures corresponds to the drift defining the damage state under consideration (in Fig. 5, 1.5%). However, since linear interpolation (between intensities and drift points in mainshock IDA) is used to determine the mainshock scale factors for bringing a building to a particular damage state for a particular ground motion, the actual damage state drift varies (e.g. in the range 1.2-1.8% in Fig. 5 (b)).

In Fig. 5 (a), aftershock IDA results show 30 mainshock-aftershock sequences all with the same mainshock ground motion (and hence all the same deterministic mainshock drift), and 30 different aftershock ground motions causing collapse. Fig. 5 (a) shows that there is a significant variability in aftershock response due to record-to-record variability in the aftershock ground motions. This result implies that, for a given level of damage experienced by a building in the mainshock, the aftershock performance varies significantly depending on the characteristics of aftershock motion. Fig. 5 (b) illustrates another scenario of mainshock-aftershock sequences with 30 different mainshocks, but the same aftershock. In this case, the aftershock IDA curves indicate more similar responses during the aftershock shaking. This observation indicates that the historical path of mainshock damage state is less important than the level of mainshock damage. However, the fact that the aftershock IDA curves are not exactly the same in Fig. 5 (b) indicates that the path to the mainshock damage also seems to play a role in determining variation in aftershock collapse capacities. Similar behavior was observed for nonlinear modern ductile MDOF building models by Raghunandan *et al.* [6] (reproduced in Fig. 5 (c) and (d)) and simplified nonlinear SDOF models by Ryu *et al.* [21].

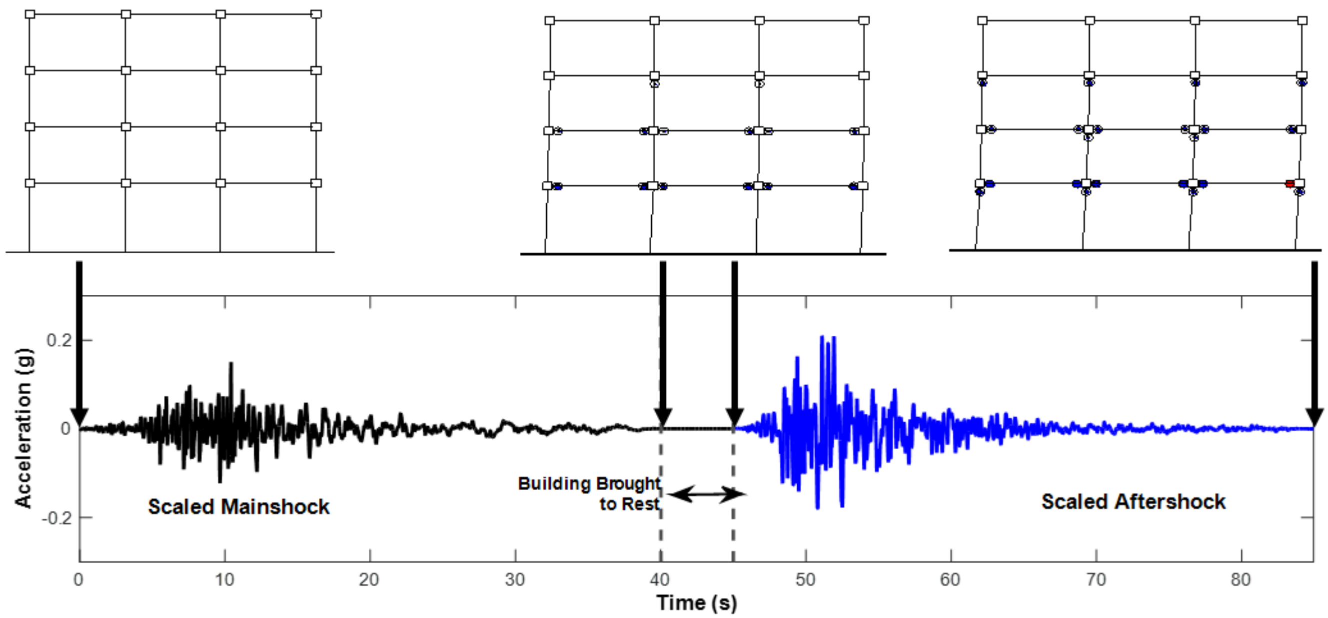

Fig. 4 –Illustration of IDA for mainshock-aftershock sequence along with an example of building response at major points in the sequence. The blue and red circles on RC frame sketch on top of ground motion sequence represent the plastic hinges for the lumped plasticity beam column element that have yielded (blue) and failed (red).

4.2 Aftershock collapse and damage fragility curves

A collapse fragility curve quantifies the probability of collapse for a building for a particular level of ground motion intensity. Fig. 6 shows the collapse fragility curves for the intact and mainshock-damaged (four damage states, DS1-4) 4-story non-ductile building. The median collapse capacity of the DS1, DS2, DS3, DS4 mainshock-damaged building, respectively, are 1%, 5%, 13.3% and 28% lower than the collapse capacity of the intact building, as summarized in Table 1. As expected, as the building becomes damaged, its capacity to withstand future shaking is reduced. Increased duration of shaking from mainshock-aftershock sequences, as compared to mainshock alone, leads to damage accumulation over the course of shaking that leads to reduction in collapse capacity of mainshock damaged building. The variability in the collapse capacity (lognormal standard deviation of the collapse fragility curve) also generally increases in the case where the building is already damaged because of the increase uncertainty in the state of the building before an aftershock occurs.

Table 1 also provides statistics for damage fragility curves, which are analogous to the collapse fragility curves, showing probability of being in a particular or worse damage state (defined as previously) as a function of ground motion intensity. The damaged building is more vulnerable to experience higher levels of damage as compared to intact buildings. This is indicated clearly by reduction in median capacity of damage fragility curves for damaged building as compared to an intact building. In fact, the level of damage sustained by the building in the mainshock greatly influences the amount of reduction in median capacity of damaged building as compared to intact building, similar to the trend observed for collapse fragility curves. For example, for the intact building, at ground motion shaking intensity corresponding to S_{di} of 5.1in, there is 50% probability that building will be in DS4 or worse (such as collapse). However, as the building incurs more damage, *i.e.* it is in DS1, DS2 or DS3, respectively, the median S_{di} for DS4 or worse becomes 5.1in, 4.8in and 4.2in.

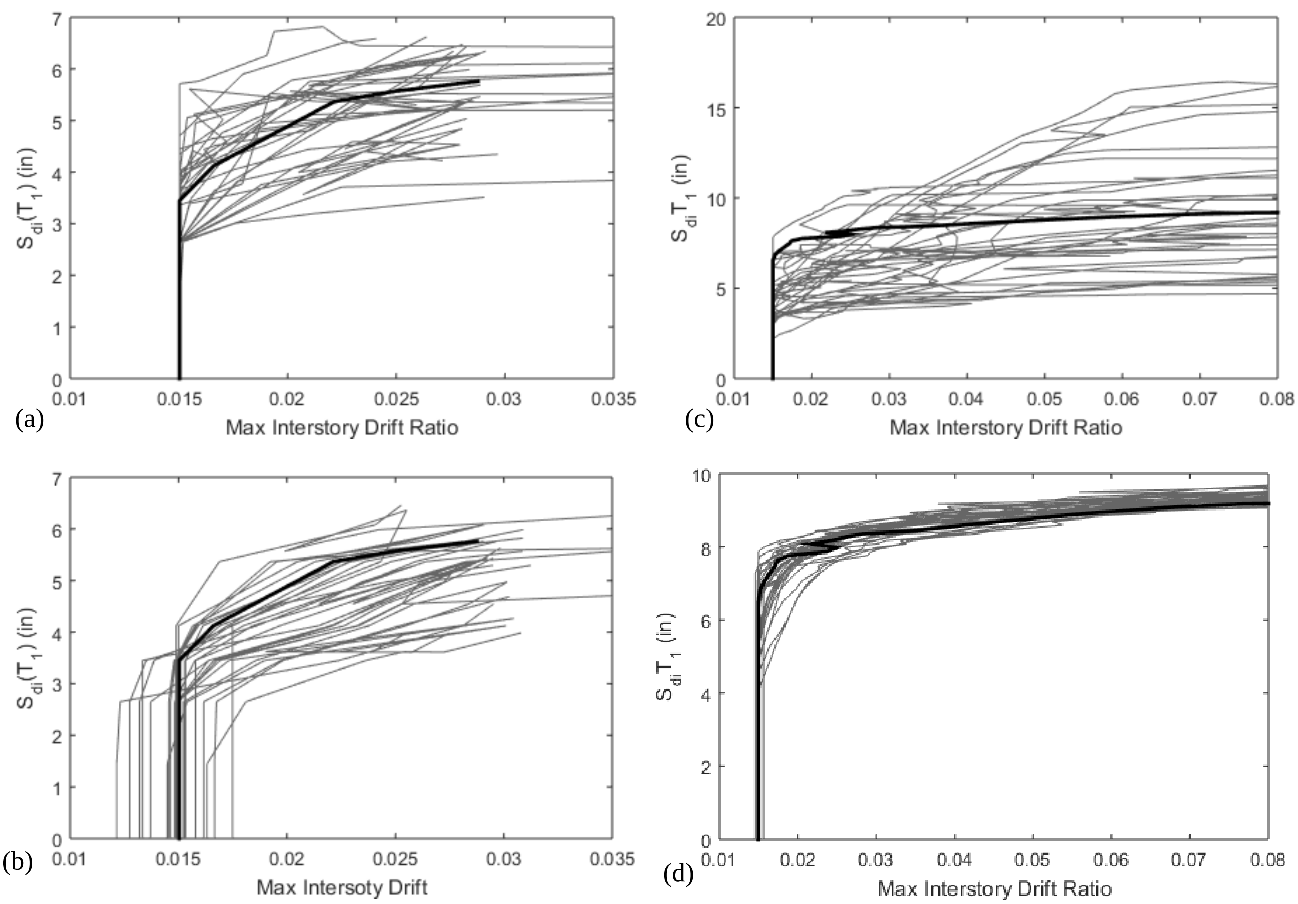

Fig. 5 – IDA results for non-ductile RC frame building showing (a) response of structure when subjected to the same mainshock record, but 30 different aftershock records, and (b) response of the structure when subjected to 30 different mainshock records, but the same aftershock record. Similarly, IDA results for ductile RC frame building showing (c) response of structure when subjected to the same mainshock record, but 30 different aftershock records, and (d) response of the structure when subjected to 30 different mainshock records, but the same aftershock record. The x-axis represents the maximum interstory drift (ISD) ratio experienced by the structure during the mainshock-aftershock sequence. The thick black line indicates the IDA results from a particular mainshock-aftershock sequence.

4.3 Comparison with the ductile RC frame building

The authors have previously conducted a similar analysis considering a 4-story ductile moment resisting frame [6], and the results are reported here in Fig. 5 (c) and (d) and Fig. 6. For the modern ductile 4-story building, a 0%, 11%, 16% and 19% reduction is observed between the median collapse capacity of intact building and DS1-DS4 mainshock-damaged building, respectively. These results show that the 2% maximum interstory drift in mainshock (DS4) may lead to extensive damage in mainshock for non-ductile building (28% lower median collapse capacity), but this damage is qualitatively less significant in ductile buildings that can sustain high maximum interstory drifts (19% lower median collapse capacity). The deformation capacity of the building also plays a significant role in the aftershock collapse vulnerability assessment of structures. As per Raghunandan *et al.* [6], for the ductile RC building, 28% reduction in median collapse capacity for damaged building will occur when the building has experienced 2.5-3% maximum interstory drift in mainshock. This same level of reduction occurs for lower mainshock damage at 2% mainshock drift for the non-ductile building analyzed here.

Fig. 7 illustrates how percentage change is collapse capacity between intact building and mainshock-damaged building varies with the level of damage sustained by the building in mainshock. The x-axis in Fig. 7 quantifies the level of mainshock damage in terms of the maximum interstory drift experienced by the building in mainshock. As per Fig. 7 and Raghunandan *et al.* [6], a gradual decrease in collapse capacity is observed over a wide range of mainshock drifts or damage levels for the ductile RC frames (~0% reduction in aftershock median collapse capacity at 0.5% drift in mainshock to 38% reduction in aftershock collapse capacity at 5% drift in mainshock). In contrast, the IDA results for the non-ductile building in Fig. 3 (a), Fig. 5 (a) and Fig. 5 (b) illustrate that the maximum drifts it can experience before it collapses is between 2.5 to 3% on average. Because of its lower deformation capacity, the non-ductile building may experience a drastic reduction in aftershock median collapse capacity at drifts higher than 2%, as indicated the steeper decline in collapse capacities for this building in Fig. 7. Therefore, it is extremely important to comprehensively understand the vulnerability of non-ductile buildings under mainshock-aftershock sequences because their low strength and deformation capacity may result in insufficient warning and protection against aftershock collapse.

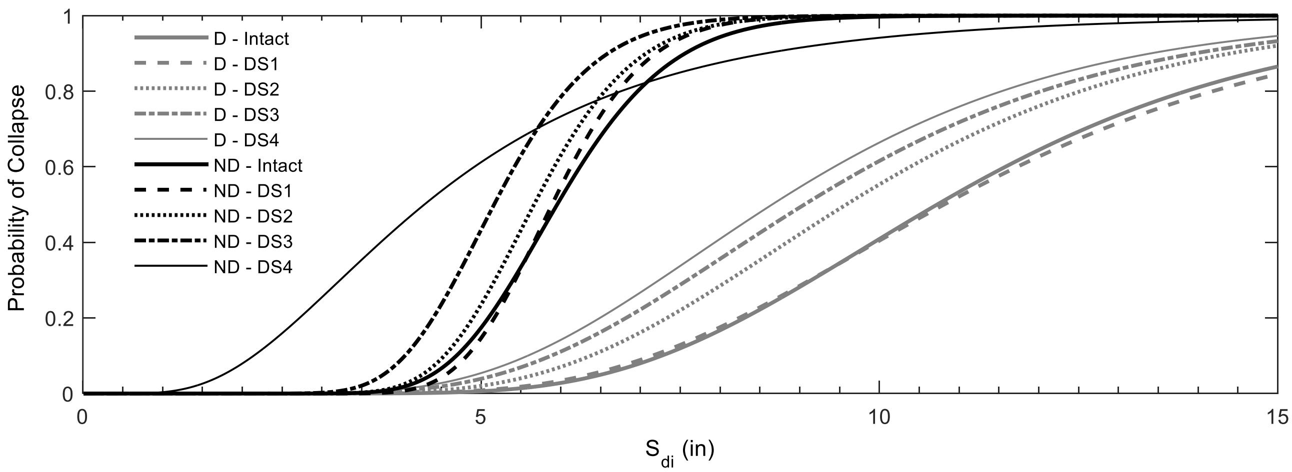

Fig. 6 – Collapse fragility curves for the four-story ductile (D) and non-ductile (ND) RC frame buildings showing the shift in collapse fragility of damaged building as a function of mainshock damage (DS1-DS4)

Table 1 – Median and lognormal standard deviation of aftershock damage and collapse fragility curves for the four-story non-ductile RC frame building for mainshock damage levels

		Aftershock Damage									
		Median S_{di}					Lognormal Standard Deviation $\sigma_{\ln S_{di}}$				
		DS1	DS2	DS2	DS4	Collapse	DS1	DS2	DS2	DS4	Collapse
Mainshock Damage	Intact	1.6	3.4	4.5	5.1	5.95	0.19	0.10	0.14	0.13	0.19
	DS1	-	3.3	4.4	5.1	5.89	-	0.11	0.15	0.14	0.16
	DS2	-	-	4.0	4.8	5.66	-	-	0.18	0.18	0.17
	DS3	-	-	-	4.2	5.16	-	-	-	0.21	0.19
	DS4	-	-	-	-	4.29	-	-	-	-	0.54

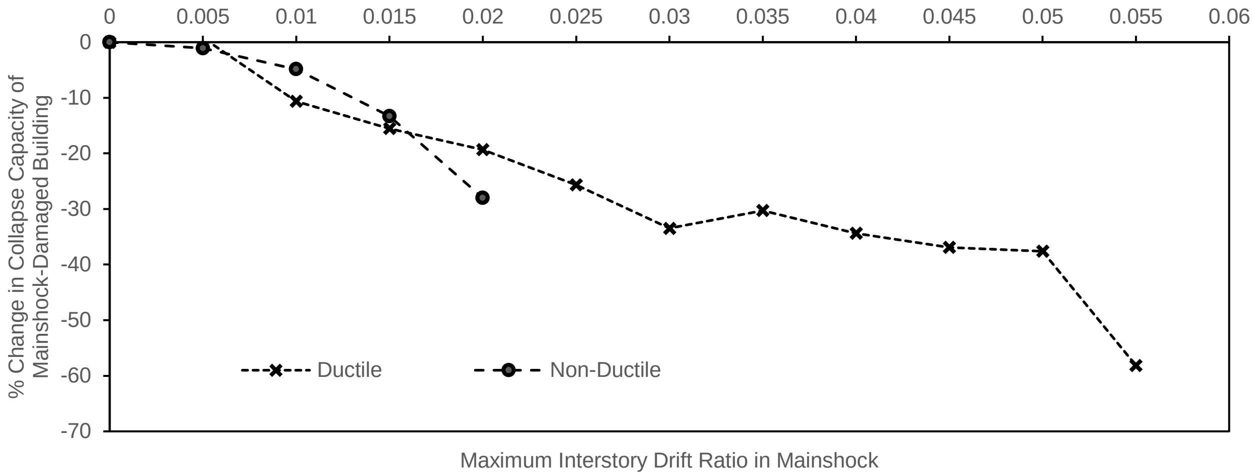

Fig. 7 – Percent change in collapse capacity of mainshock-damaged buildings from intact building for different levels of mainshock damage sustained by the building. Mainshock damage is quantified in terms of maximum interstory drift ratio of the building in mainshock.

5. Conclusions

This study examines the capacity of a non-ductile RC frame, of the type existing among older buildings in California, New Zealand and around the world, to withstand damage and collapse if it is already damaged. The analysis consists of applying a large number of mainshock-aftershock sequences to a nonlinear simulation model of the building to examine collapse fragility in the context of existing mainshock damage. Results show, as expected, that the collapse capacities decrease as the building is more severely damaged in the mainshock. The building also becomes more likely to incur more significant damage for a given intensity of aftershock shaking, if it has experienced some mainshock damage. The results also show that the drop in capacity is more precipitous for the non-ductile RC frame building than for a comparable modern ductile RC seismically-designed moment frame, indicating the importance of carefully evaluating and tagging these buildings after an earthquake.

6. References

[1] USGS (2014): United States Geological Survey.

[2] Hatzigeorgiou GD, Liolios AA (2010): Nonlinear behaviour of RC frames under repeated strong ground motions. *Soil Dynamics & Earthquake Engineering*, **30**(10), 1010-1025.

[3] Tesfamariam S , Goda K, Mondal G (2015): Seismic vulnerability of RC frame with unreinforced masonry infill due to mainshock-aftershock earthquake sequences. *Earthquake Spectra*, **31**(3), 1427-1449.

[4] Nazari N, van de Lindt J, Li Y (2015): Effect of Mainshock-aftershock sequences on woodframe building damage fragilities. *Journal of Performance of Constructed Facilities*, **29**(1).

[5] Raghunandan M and Liel AB (2013): Effect of ground motion duration on earthquake-induced structural collapse," *Structural Safety*, **41**, 119-133.

[6] Raghunandan M, Liel AB, Luco N (2015): Aftershock collapse vulnerability assessment of reinforced concrete frame structures. *Earthquake Engineering & Structural Dynamics*, **44**(3), 419-439.

[7] Liel AB, Haselton CB, and Deierlein GG (2011): Seismic collapse safety of reinforced concrete buildings II: comparative assessment of nonductile and ductile moment frames. *Journal of Structural Engineering*, **137**(4), 492-502.

[8] Marquis F, Kim JJ, Elwood KJ, and Chang SE (2015): Understanding post-earthquake decisions on multi-storey concrete buildings in Christchurch, New Zealand. *Bulletin of Earthquake Engineering*, 1–28.

[9] Raghunandan M, Liel AB, Ryu H, and Luco N (2012): Aftershock Fragility Curves and Tagging Assessments for a Mainshock-Damaged Building. *15 WCEE,* Lisbon,Portugal.

[10] Elwood KJ (2004): Modelling failures in existing reinforced concrete columns. *Canadian Journal of Civil Engineering*, **31**(5), 846-859.

[11] OpenSees (2014): Open System for Earthquake Engineering Simulation.

[12] Ibarra LF, Medina RA, and Krawinkler H (2005): Hysteretic models that incorporate strength and stiffness deterioration. *Earthquake Engineering & Structural Dynamics*, **34**(12), 1489-1511.

[13] Sezen H, and Moehle J (2004): Shear Strength Model for Lightly Reinforced Concrete Columns. *Journal of Structural Engineering*, **130**(11), 1692-1703.

[14] Raghunandan M, Liel AB, and Luco N (2014): Collapse Risk of Buildings in the Pacific Northwest Region due to Subduction Earthquakes. *Earthquake Spectra*, **31**(4), 2087-2115.

[15] Haselton CB, Liel AB, Deierlein GG, Dean BS, and Chou JH (2011): Seismic Collapse Safety of Reinforced Concrete Buildings. I: Assessment of Ductile Moment Frames. *Journal of Structural Engineering*, **137**(4), 481-491.

[16] Porter KA, Kiremidjian AS, and LeGrue JS (2001): Assembly-Based Vulnerability of Buildings and Its Use in Performance Evaluation. *Earthquake Spectra*, **17**(2), 291–312.

[17] Vamvatsikos D and Cornell CA (2006): Direct estimation of the seismic demand and capacity of oscillators with multi-linear static pushovers through IDA. *Earthquake Engineering & Structural Dynamics*, **35**(9), 1097-1117.

[18] Ruiz-García J, Negrete-Manriquez JC (2011): Evaluation of drift demands in existing steel frames under as-recorded far-field and near-fault mainshock–aftershock seismic sequences. *Engineering Structures*, **33**(2), 621–634.

[19] Tothong P, Luco N (2007): Probabilistic seismic demand analysis using advanced ground motion intensity measures. *Earthquake Engineering & Structural Dynamics*, **36**(13), 1837–1860.

[20] Baker JW and Cornell CA (2006): “Spectral shape, epsilon and record selection,” *Earthquake Engineering & Structural Dynamics*, **35**(9), 1077–1095.

[21] Ryu H, Luco N, Uma SR, Liel AB (2011): Developing fragilities for mainshock-damaged structures through incremental dynamic analysis,” *9PCEE Paper No.* 225, Auckland, New Zealand.